

See discussions, stats, and author profiles for this publication at: <https://www.researchgate.net/publication/15649864>

A Predictive Substrate Model for Rat Glutathione S-Transferase 4-4

ARTICLE *in* CHEMICAL RESEARCH IN TOXICOLOGY · JULY 1995

Impact Factor: 3.53 · DOI: 10.1021/tx00047a004 · Source: PubMed

CITATIONS

11

READS

5

7 AUTHORS, INCLUDING:



[Peter Nieuwenhuizen](#)

AkzoNobel

29 PUBLICATIONS 422 CITATIONS

[SEE PROFILE](#)



[Jan N.M. Commandeur](#)

VU University Amsterdam

204 PUBLICATIONS 4,886 CITATIONS

[SEE PROFILE](#)

A Predictive Substrate Model for Rat Glutathione S-Transferase 4-4

Marcel J. de Groot,^{†,‡} Ellen M. van der Aar,[†] Peter J. Nieuwenhuizen,^{†,‡}
R. Martijn van der Plas,[‡] Gabriëlle M. Donné-Op den Kelder,^{†,‡}
Jan N. M. Commandeur,[†] and Nico P. E. Vermeulen^{*,†}

Leiden/Amsterdam Center for Drug Research, Divisions of Molecular Toxicology and Medicinal Chemistry, Department of Pharmacochemistry, Vrije Universiteit, De Boelelaan 1083, 1081HV Amsterdam, The Netherlands

Received October 27, 1994[§]

Molecular modeling techniques have been used to derive a substrate model for class mu rat glutathione S-transferase 4-4 (GST 4-4). Information on regio- and stereoselective product formation of 20 substrates covering three chemically and structurally different classes was used to construct a substrate model containing three interaction sites responsible for Lewis acid–Lewis base interactions (IS_1 , IS_2 , and IS_3), as well as a region responsible for aromatic interactions (IS_4). Experimental data suggest that the first protein interaction site (pIS_1 , interacting with IS_1) corresponds with Tyr¹¹⁵, while the other protein interaction sites (pIS_2 and pIS_3) probably correspond with other Lewis acidic amino acids. All substrates exhibited positive molecular electrostatic potentials (MEPs) near the site of conjugation with glutathione (GSH), as well as negative MEP values near the position of groups with Lewis base properties (IS_1 , IS_2 , or IS_3), which interact with pIS_1 , pIS_2 , or pIS_3 , respectively. Obviously, complementarity between the MEPs of substrates and protein in specific regions is important. The substrate specificity and stereoselectivity of GST 4-4 are most likely determined by pIS_1 and the distance between the site of GSH attack and Lewis base atoms in the substrates which interact with either pIS_2 , pIS_3 , or a combination of these sites. Interaction between aromatic regions in the substrate with aromatic amino acids in the protein further stabilizes the substrate in the active site. The predictive value of the model has been evaluated by rationalizing the conjugation to GSH of 11 substrates of GST 4-4 (representing 3 classes of compounds) which were not used to construct the model. All known metabolites of these substrates are explained with the model. As the computer-aided predictions appear to correlate well with experimental results, the presented substrate model may be useful to identify new potential GST 4-4 substrates.

Introduction

Glutathione S-transferases (GSTs; EC 2.5.1.18)¹ catalyze the nucleophilic attack of the tripeptide glutathione (GSH) to electrophilic substrates, which results in addition or substitution reactions, depending on the nature of the substrate (1). The primary function of these enzymes is generally considered to be detoxification of both endogenous and xenobiotic compounds (1, 2). Most GST isoenzymes can accommodate a broad range of electrophilic substrates: the substrate selectivity is low. The stereoselectivity of the isoenzymes, however, is relatively high (3).

Mammalian cytosolic GST isoenzymes have been classified into four families, alpha, mu, pi, and theta (4, 5), and can be distinguished via their molecular masses, isoelectric points, and other properties. GSTs are found as dimeric proteins comprised of two subunits (6). Both homodimers and heterodimers can be formed, while heterodimers can only be formed between subunits of the same family. The primary sequence homology between subunits of the same family is >70%, while interfamily subunit homologies are approximately 30–40% (1, 7). Each isoenzyme subunit contains an active site consisting of two binding sites, one for the cofactor GSH (G-site) and one for the electrophilic substrate (H-site) (6, 8).

Only 60% of the Caucasian population possesses human class mu GST 1-1, which has a high catalytic activity (together with human class pi GST isoenzymes (3)) in the conjugation of many potentially toxic and carcinogenic alkene and arene oxides, such as styrene 7,8-oxide, benzo[a]pyrene 4,5-oxide, and benzo[a]pyrene 7(R),8(S)-diol 9(S),10(R)-epoxide (9, 10). The polymorphism of this isoenzyme is genetically determined and is caused by the absence of the GST 1 allele. Homozygous individuals for this null allele display a very low activity, or a complete absence of activity with respect to conjugation of *trans*-stilbene oxide (10–12). Human GST 1-1 and rat GST 4-4 show a high homology in primary amino acid sequence (88%),² and this may implicate a high similarity in substrate selectivity (3, 13).

* To whom correspondence should be addressed.

[†] Division of Molecular Toxicology.

[‡] Division of Medicinal Chemistry.

[§] Abstract published in *Advance ACS Abstracts*, May 1, 1995.

¹ Abbreviations: BPDE, benz[a]pyrene 7,8-diol 9,10-epoxide; CNDN, 1-chloro-2,4-dinitrobenzene; CSD, Cambridge Structural Database; ΔE , energy difference between minimal energy conformation and fitted conformation; $\Delta E_{eq,ax}$, energy difference between the diequatorial and the diaxial conformation; ΔG , Gibbs free energy difference; ΔH , enthalpy difference; DMA, distributed multipole analysis; ΔS , entropy difference; GAMESS-UK, Generalised Atomic and Molecular Electronic Structure System UK-version; GS^- , glutathione anion; GST, glutathione S-transferase; IS, interaction site in the substrate, which interacts with a corresponding pIS in the enzyme; MEP, molecular electrostatic potential; PBO, 4-phenyl-3-butene-2-one; pIS , protein interaction site in the protein, responsible for interaction with a corresponding IS in the substrate; RHF, restricted Hartree Fock; r_{vdw} , van der Waals radius; STO, Slater type orbital; SV, split valence.

Xenobiotic and endogenous compounds shown to be conjugated by GST 4-4 comprise aromatic epoxides (14–19), aromatic halides (1, 20, 21), α,β -unsaturated ketones (1, 22), and (α -bromoisovaleryl)urea (23). Most known substrates of GST 4-4 contain aromatic or conjugated regions near the GSH conjugation site.

Until now only simple and descriptive models for conjugation by GST isoenzymes have been described. One model is based on the stereoselectivity of GSH conjugation of some aromatic and aliphatic oxiranes (19, 24). Dostal *et al.* indicated a hydrophobic interaction to be a determinant for the stereoselectivity of conjugation of the aromatic and aliphatic epoxides to GSH in rat cytosol (24), while Cobb *et al.* attributed the stereoselectivity of rat subunit 4 to positioning of a critical acid, required for protonation of the leaving group, or to asymmetry in the hydrophobic surface of the substrate binding site (19). Another model is based on the stereochemistry of conjugation of α -bromoisovaleric acid and (α -bromoisovaleryl)urea to GSH (23). Both hydrophobic interactions and hypothetical hydrogen bridges to polar groups in the active site were suggested to be important for binding and orientation of (α -bromoisovaleryl)urea. Polar and/or hydrophobic interactions within the H-site of various isoenzymes were suggested to be responsible for the observed stereoselective metabolism (23). However, as (α -bromoisovaleryl)urea has only a very low affinity for GST 4-4 ($K_m > 10$ mM) and a limited water solubility (≈ 7 mM), no reliable K_m and v_{max} values have been determined (23); therefore, the reliability of this (α -bromoisovaleryl)urea based model cannot be judged.

The primary aim of the present study was to derive and validate, if possible, a predictive substrate model for GST 4-4, on the basis of a wide range of known substrates. The substrate model was derived on the basis of 20 substrates and validated by rationalizing the conjugation of 6 substrates of GST 4-4 to GSH not used to construct the model. Furthermore, predictions were done for a series of 5 compounds known to be conjugated by GST 4-4 for which the absolute configuration of the products (two diastereomers) is unknown.

Methods

Biological Data. The experimental data on stereoselective product formation and Michaelis–Menten constants (K_m) used to construct and verify the substrate model were derived from literature and experiments performed at our own laboratories using purified GST 4-4.³ The structures of the compounds used in this study are given in Charts 1a–c, 2, and 3.

Computational Data and Molecular Modeling. The initial conformations of 1-chloro-2,4-dinitrobenzene (CDNB) (4), 1,2-dichloro-4-nitrobenzene (5), benzo[*a*]pyrene (as starting conformation for benzo[*a*]pyrene 7,8-diol 9,10-epoxide (BPDE)), and 2-cyano-1,3-dimethyl-1-nitrosoguanidine (26) were retrieved from the Cambridge Structural Database (CSD (25)). The initial conformations of the other substrates (Charts 1a–c, 2, and 3) were generated using the molecular modeling package Chem3D (26).

² Homology determined by aligning sequences GTB1_rat (rat class mu GST 3-3), GTB2_rat (rat class mu GST 4-4), and GTM1_human (human class mu GST 1-1) retrieved from the Swiss-Protein Database using the PSQ routines of the CAMMSA program package (George, D. G., and Barker, W. C. (1989) PSQ User's Guide, Protein Identification Resource, National Biomedical Research Foundation, Georgetown, University Medical Center, Washington; and Leunissen, J. A. M., Vergert, H. M. ter, and Gelder, C. W. G. van (1990) CAMMSA User Manual, Version 1.0, CAOS/CAMM Center, University of Nijmegen, Nijmegen, The Netherlands).

³ E. M. van der Aar *et al.*, unpublished results.

Chart 1. Substrates of GST 4-4 Used in This Study To Build the Substrate Model: (a) Aromatic Diol Epoxides, (b) Substituted Aromatic Chlorides, and (c) Pyrene Oxide and (Aza)phenanthrene Oxides

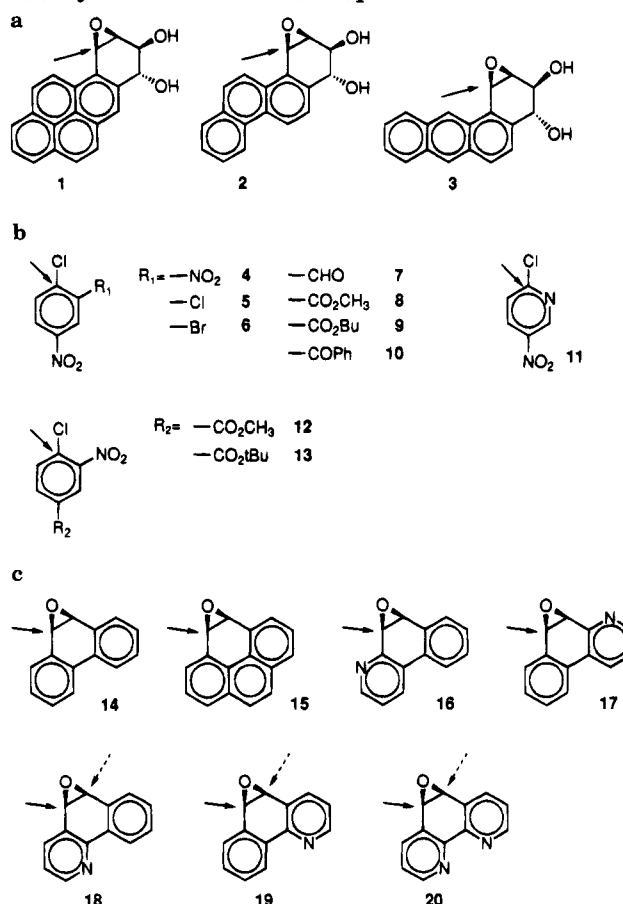


Chart 2. Substrates of GST 4-4 Used in This Study To Verify the Substrate Model: Stilbene Oxides, Styrene Oxides, and 2-Cyano-1,3-dimethyl-1-nitrosoguanidine

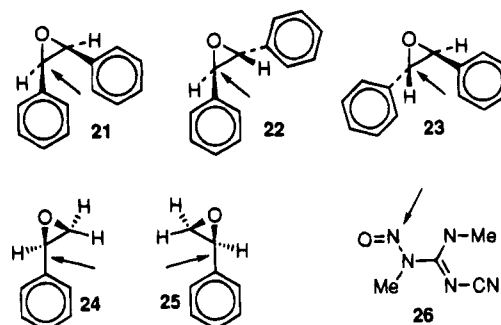
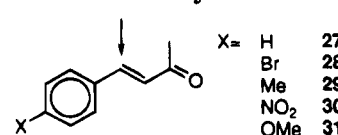


Chart 3. Compounds Predicted To Be Conjugated by GST 4-4 Based on the Substrate Model: Substituted 4-Phenyl-3-buten-2-ones



The quantum chemical program package GAMESS-UK (27, 28), implemented on IBM/RS6000 workstations and on a CRAY-YMP supercomputer, was used for the *ab initio* calculations described. The geometries of all substrates were *ab initio* optimized at the RHF (restricted Hartree Fock) level using the STO-3G (Slater type orbital comprised of 3 Gaussians) (29) minimal basis set. On the resulting STO-3G geometries, a

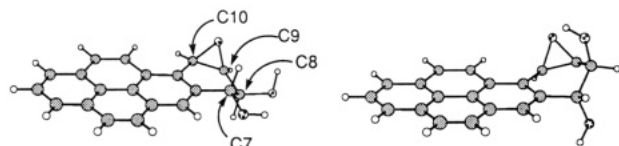


Figure 1. Diequatorial (left) and diaxial (right) conformation of template molecule BPDE (**1**).

single point energy calculation and DMA (distributed multipole analysis) calculation (30) were performed using the RHF method in a SV (split valence) 6-31G (31, 32) basis set.⁴ For the epoxides **1–3**, the aldehyde **7**, the esters **8, 9, 12**, and **13**, the ketone **10**, and the nitrosoguanidine compound **26**, various possible low energy conformations were investigated with *ab initio* methods.

To build a substrate model, benzo[*a*]pyrene 7(*R*),8(*S*)-diol 9(*S*),10(*R*)-epoxide (**1**) was chosen as a template molecule. The two low energy conformations of **1** are indicated in Figure 1. The molecular modeling program ChemX (26) was used for rigid and flexible fitting. In the rigid fitting procedure, compounds are fitted onto the template molecule only allowing global rotations and translations. The flexible fitting minimizer uses the ChemX nonbonded energy force field. In the flexible fitting procedure also user-defined exocyclic dihedral angles are minimized with respect to restraints set by the user on the one hand, and the nonbonded energy of the fitted molecule on the other hand. All substrates were fitted onto **1** with the rigid fitting procedure, when necessary followed by a flexible fitting procedure (26). The sites of GSH attack in the different substrates were matched onto each other. Furthermore, the various functional groups of the substrates were fitted onto the functional groups of the template molecule, such that the charges of the matched atoms were similar, assuming a similar environment for each substrate in the active site. When the distance between fitted atoms was less than 0.25 Å, the fitted conformation was accepted. The energy of the fitted conformation was calculated with *ab initio* methods (RHF/SV 6-31G (31, 32)). When the energy difference between the minimal energy conformation and the fitted conformation was less than 21 kJ/mol (5 kcal/mol), the fitted conformation was finally accepted and a distributed multipole analysis (DMA (30)) was carried out.

Molecular electrostatic potentials (MEPs) based on Coulomb point charge interactions between the compound and a positive charge were calculated with ChemX (33) on the van der Waals surface for a series of compounds using partial atomic charges derived from the *ab initio* DMA calculations (monopoles only (30)).

Results and Discussion

The primary aim of the present study was to derive a substrate model for GST 4-4, on the basis of a wide variety of known substrates, and to evaluate its ability to rationalize conjugation reactions catalyzed by GST 4-4. The substrate model was constructed using three series of known substrates of GST 4-4: aromatic diol epoxides, activated aromatic chlorides, and (aza)arene oxides (Chart 1a–c and Table 1). The substrate model derived was evaluated by rationalizing the conjugation of substrates of GST 4-4 to GSH not used to derive the model (Chart 2 and Table 2). Furthermore, predictions were made for some substrates of which GSH conjugation is known to be catalyzed by GST 4-4 with unknown absolute configurations in the conjugates (Chart 3 and Table 3).

Selection of the Template Molecule. To build a substrate model, BPDE was chosen as a template molecule as it is one of the largest substrates known to be efficiently conjugated by GST 4-4. The conjugation of

Table 1. Computational and Experimental Data of GST 4-4 Substrates Used To Build the Substrate Model

	d_1 (Å) ^a	d_2 (Å) ^b	ΔE (kJ/mol) ^c	% <i>R</i> ^d
1	3.8	4.3	0.0	98 (14)
2	3.8	4.3	0.0	97 (14)
3	3.8	4.3	0.0	95 (14)
4	3.6		0.0	
5	2.8		0.0	
6	2.9		0.0	
7	3.7		0.0	
8	3.7		5.93	
9	3.7		5.96	
10	3.7		31.63	
11	1.3		0.0	
12	3.6		0.0	
13	3.6		0.0	
14			0.0	>99 (17)
15			0.0	>99 (17)
16			0.0	96 (17)
17			0.0	96 (17)
18		(S) ^e 4.3	0.0	73 (17)
19	(S) ^e 3.8		0.0	89 (17)
20		(R) ^e 4.3	0.0	78 (17)
	(S) ^e 3.8	(S) ^e 4.3		

^a Distance between site of GSH attack and Lewis base (IS₂) interacting with pIS₂. ^b Distance between site of GSH attack and Lewis base (IS₃) interacting with pIS₃. ^c Energy differences between the minimal energy conformation and the conformation of the compound in the model. ^d Stereospecificity of conjugation (% of conjugation at the carbon atom of the epoxide moiety with *R*-stereochemistry). ^e (S) or (R): fit explaining conjugation at carbon atom with S- or R-stereochemistry.

Table 2. Computational Data of GST 4-4 Substrates Used To Verify the Substrate Model^a

substrate	d_1 (Å)	ΔE (kJ/mol)	substrate	d_1 (Å)	ΔE (kJ/mol)
21		5.31	25		0.0 ^b
22		5.49	26	3.6	0.0
23	0.0 ^b		26	3.7	16.1
24		6.02			

^a For an explanation of d_1 and ΔE , see the legend to Table 1. ^b Fit in the model could not be improved by changing the geometry.

Table 3. Computational and Experimental Data of Substrates Conjugated by GST 4-4 with Unknown Absolute Configuration of the GSH Conjugates^a

substrate	d_1 (Å)	ΔE (kJ/mol) ^b	% A ^c	substrate	d_1 (Å)	ΔE (kJ/mol) ^b	% A ^c
27	3.6	0.0	90 (22)	30	3.6	0.0	66 (22)
28	3.6	0.0	84 (22)	31	3.6	0.0	95 (22)
29	3.6	0.0	93 (22)				

^a For an explanation of d_1 and ΔE , see the legend to Table 1.

^b Compared to the global minimum (*cis*), the energy is 6.0 kJ/mol higher. ^c % GSH conjugate stereoisomer A (absolute configuration unknown (22)).

BPDE by GST 4-4 to GSH is well-defined and highly stereoselective for attack of GSH at the *R*-configured carbon atom (Figure 1: C₁₀) of the epoxide ring for the 7*R*,8*S*,9*S*,10*R*-stereoisomer **1** (14, 15). This indicates either that the 7*R*,8*S*,9*S*,10*R*-stereoisomer of BPDE (**1**) will bind in a very specific orientation in the active site of GST 4-4 or that the reaction intermediate of this enantiomer is more stabilized than the intermediates of the other 3 stereoisomers. Furthermore, **1** has a high affinity for GST 4-4 (14), it is semirigid because it has little conformational freedom, and it has three polar, functional groups (one epoxide and two hydroxyl groups) and an aromatic region which might be involved in the orientation and binding of the substrate in the active site.

Two conformations of **1** were considered, namely, those in which the C₇- and C₈-hydroxyl groups were either in

^a Due to unavailability of a SV 6-31G basis set for bromine, a SV 3-21G basis set was used.

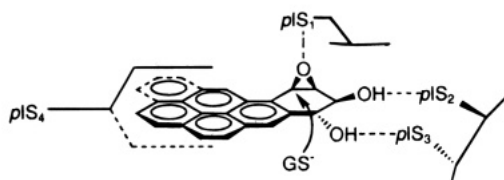


Figure 2. Substrate model for the active site of GST 4-4. Epoxide oxygen atom (IS_1), C_8 -hydroxyl group (IS_2), and C_7 -hydroxyl group (IS_3), interacting with protein interaction sites (pIS_1 , pIS_2 , and pIS_3 , respectively), and aromatic interaction region (IS_4) interacting with aromatic amino acids in the protein (pIS_4).

a diaxial or in a diequatorial orientation. The two low energy conformations of **1** are indicated in Figure 1. Both conformations were *ab initio* optimized and their energies compared. The diequatorial conformation was favored by 6.3 kJ/mol. When using $\Delta G^\circ = -RT \ln(k_{eq}/k_{ax})$, the calculated ΔG° ($\Delta G^\circ \approx \Delta E_{eq-ax}$ when assuming $\Delta H^\circ \approx \Delta E_{eq-ax}$ and $\Delta S^\circ \approx 0$) of -6.3 kJ/mol then corresponds to an equilibrium distribution of 92% diequatorial and 8% diaxial at 311 K (34). This energy difference (ΔE_{eq-ax}) is too small to conclusively select the diequatorial conformation as the most likely template conformation *a priori*. Therefore, initially both the (lower energy) diequatorial and the (higher energy) diaxial conformations were used to fit a selection of substrates (aromatic diol epoxides, aromatic chlorides, and (aza)arene oxides). This gave acceptable fits, however, only when the diequatorial conformation was used (diazial data not shown). Based on these initial data, the diequatorial conformation of **1** was chosen as template.

Aromatic Diol Epoxides (Chart 1a: 1–3). The aromatic diol epoxides **1–3** have been reported to be conjugated with high stereoselectivity (95–98%) by GST 4-4 at the *R*-configured carbon atom of the epoxide moiety (14). The conjugation is considered to be an S_N2 reaction, with the epoxide oxygen serving as intramolecular leaving group. This reaction requires substrate binding to occur with the oxirane ring orientated in a position for *trans*-antiparallel attack by the thiolate anion (GS^-) as nucleophile, as reported for oxiranes and (aza)arene oxides (19).

As expected, the diequatorial conformation of **2** and **3** fitted exactly onto the diequatorial conformation of **1**. For **1–3**, the energy difference between the diequatorial and the diaxial conformations (ΔE_{eq-ax}) was calculated to be about 6 kJ/mol, which is in agreement with the experimentally determined ΔE_{eq-ax} of 3 kJ/mol per hydroxyl group (35). Our calculations revealed no significant differences in the partial atomic charges of the two carbon atoms of the oxirane moiety for neither of the three diol epoxides (data not shown). As the conjugation of GSH to **1**, **2**, and **3** occurs with high stereoselectivity at the *R*-configured carbon atom (14), the direction of attack by GSH seems to be rigidly set. The epoxide oxygen atom probably has an interaction with the enzyme, assisting in orientating the substrate relative to GSH and stabilizing the intermediate conjugate. The epoxide oxygen-interaction site was designated interaction site 1 (IS_1) with a complementary hypothetical protein interaction site (pIS_1 ; Figure 2) in the active site of the protein. Additional interaction may be present between the aromatic part of these substrates (IS_4) and aromatic amino acids in the protein (pIS_4 ; Figure 2), thus assisting in orientating the substrates in a specific way; the latter interaction site (IS_4) was designated the aromatic interaction region.

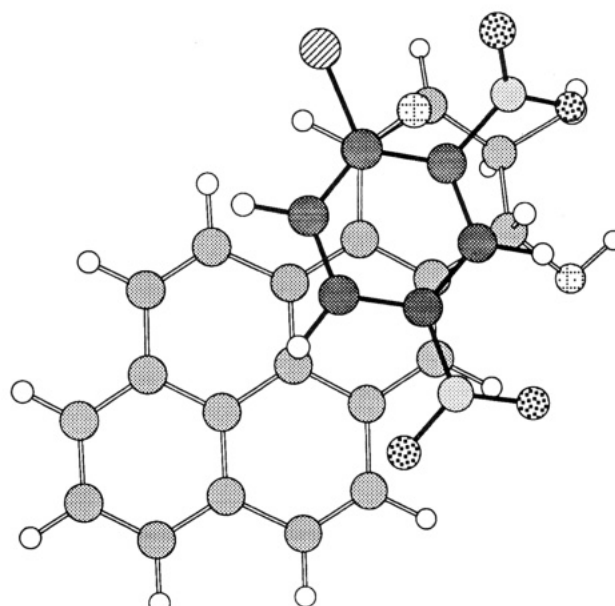


Figure 3. Fit of CDNB (4) in the substrate model.

Aromatic Chlorides (Chart 1b: 4–13). The aromatic chloride **4** is a well-known substrate for most GST isoenzymes (3). Conjugation takes place via nucleophilic aromatic substitution of the chlorine atom by GSH. This requires activation of the aromatic ring through electron-withdrawing substituents, stabilizing the intermediate Meisenheimer complex (1). For a series of 1-halo-2-nitro-4-substituted-benzenes, formation of the Meisenheimer complex was shown to be partially rate limiting (1, 20, 21). Both GST 3-3 and GST 4-4 appear to have a relative high affinity for these substrates.³

Both **4** and **5** are well-known substrates of GST 4-4 and were fitted onto **1**, matching the respective sites of attack by GSH. One of the oxygen atoms of the *o*-nitro group of **4** fitted well onto the C_8 -hydroxyl oxygen atom of **1** (Figure 3). An interaction between one of the oxygen atoms of the *o*-nitro group of **4** (Lewis base) with a hypothetical Lewis acid on the enzyme might thus be postulated. The atom in the substrates (an oxygen atom in substrates **1** and **4**) responsible for this interaction was designated interaction site 2 (IS_2) with a corresponding hypothetical protein interaction site (pIS_2 ; Figure 2) in the active site of the protein. In compound **5**, the *o*-chlorine atom might also interact with pIS_2 via a Lewis acid–base interaction. The calculated distance between the conjugation site and *o*-chlorine atom of **5** is 2.8 Å, which is about 0.9 Å shorter than the corresponding average distance of 3.7 Å in compounds **1** and **4**. This would indicate a slightly larger distance between the Lewis base position in the substrate (IS_2) and the hypothetical Lewis acid position in the protein (pIS_2) for **5** when compared to **1** and **4**. The ortho substituent may not only be important for binding but also for activating substrates toward nucleophilic aromatic substitution, as the electron-withdrawing capacity of an ortho substituent can be enhanced by interaction with a Lewis acid during formation of the Meisenheimer complex (21). This difference in distance between site of conjugation and the Lewis basic atom in the substrate might to some extent contribute to the enhanced K_m of **5** ($855 \pm 107 \mu\text{M}$)³ relative to the K_m of **4** ($156 \pm 36 \mu\text{M}$).³

To substantiate the importance of IS_2 , a number of substrate analogues of **4**, notably **6–11**, were prepared, and the K_m toward GST 4-4 was determined.³ Some of

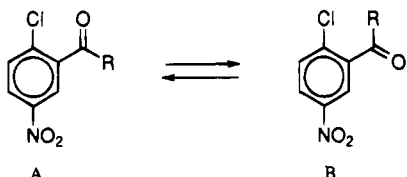
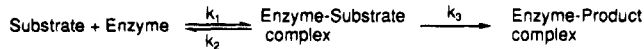


Figure 4. Low energy conformations of 1-chloro-4-nitrobenzenes with ketone or ester substituents on the 2-position.

Scheme 1. Rate Constants of the Conjugation Reaction



the aromatic chlorides (i.e., **6**, **7**, and **11**) could be fitted onto the template molecule in their minimal energy conformations. For compound **6**, a lower K_m value ($381 \pm 70 \mu\text{M}$)³ was found than for **5** ($855 \pm 107 \mu\text{M}$).³ Due to the increased size of the bromine atom ($r_{\text{vdw}} = 1.83 \text{ \AA}$) when compared to the chlorine atom ($r_{\text{vdw}} = 1.69 \text{ \AA}$), a better interaction between IS₂ and *p*IS₂ for bromine than for chlorine is anticipated.

The *o*-methyl ester and *o*-butyl ester analogues (**8** and **9**, respectively) and the benzophenone analogue **10** could not be fitted on the template in their minimal energy conformation, schematically depicted in Figure 4 as conformation A, in which the *o*-carbonyl oxygen atom is lying approximately in the plane of the aromatic ring for **7-9**, but not for **10** ($\tau = 74.5^\circ$). The conformation in which **8**, **9**, and **10** have been fitted onto **1** is schematically depicted in Figure 4 as conformation B, i.e., by superimposing the carbonyl oxygen atom of the substrates onto IS_2 . Except for compound **10**, the energy difference between the fitted and the minimal energy conformation (see ΔE 's in Table 1) is less than 21 kJ/mol (5 kcal/mol). In general, compounds from this series with Lewis base properties at a distance of approximately 3.7 Å (e.g., **4**) from the conjugation site (d_1 in Table 1) and a lower ΔE value have a low K_m value compared to compounds from this series in which the corresponding distance is smaller (e.g., **5**). Discrepancies might also be a result of differences in k_3 (Scheme 1) of different compounds.

The K_m of the pyridine analogue **11** ($1219 \pm 164 \mu\text{M}$)³ is high compared to the other K_m values within the series. This is apparently related to the relative large distance between the Lewis base nitrogen atom in the substrate (IS_2) and the hypothetical Lewis acid ($p\text{IS}_2$) in the active site of the protein. A certain correlation therefore seems to exist between the quality of the fit and the observed Michaelis-Menten constant. This suggests that the interaction between IS_2 and $p\text{IS}_2$ is of importance for binding and/or activation. It has to be realized, however, that the different electronic states of the atoms interacting with $p\text{IS}_2$ can also explain the observed differences in K_m . For **11**, the different lipophilicity compared to that of the other aromatic chlorides might also play a role.

To probe steric restrictions of the active site of GST 4-4, methyl 4-chloro-3-nitrobenzoate (**12**) and *tert*-butyl 4-chloro-3-nitrobenzoate (**13**) were synthesized and the K_m values determined.³ Substrate **12** was conjugated to GSH ($K_m = 262 \pm 101$),³ while **13** was not conjugated at all.³ Apparently, a large bulky substituent at the position para relative to the chlorine cannot be accommodated in the active site of GST 4-4, while smaller substituents can. Substrate **12** can be fitted in two conformations (see Figure 4A and 4B for the ortho position), and apparently

it can be accommodated in either of the two conformations. Based on the differences of conjugation between **12** and **13**, it seems evident that a steric factor has to be taken into account in the plane under the saturated ring of **1**.

Pyrene Oxide and (Aza)phenanthrene Oxides

(Chart 1c: 14–20). Phenanthrene 9,10-oxide (**14**), pyrene 4(*R*),5(*S*)-oxide (**15**), and azaphenanthrene oxides **16–20** are also conjugated to GSH by GST 4-4 (**17**). All 7 substrates were shown to be conjugated primarily at the benzylic carbon atom of the epoxide moiety with the *R*-configuration. The stereoselectivity of the conjugation reaction varied from 73% to >99% (Table 1). The highly stereoselective conjugation at the *R*-configured carbon atom of the epoxide moiety (*R*-fit) of **14–17** can be rationalized by fitting the epoxide moiety of **14** onto that of **1**. This supports the role of *pIS*₁ for orientating epoxide-containing substrates. Compound **18** is preferentially (73%) conjugated at the *R*-configured carbon atom but also for 27% at the *S*-configured carbon atom. The distance between the *S*-configured benzylic carbon atom and the Lewis base nitrogen atom of **18** is 4.3 Å, which is identical to the distance between the site of GSH attack of template molecule **1** and the 7-hydroxyl oxygen atom in **1**. We, therefore, hypothesize another Lewis acid group in the active site of the protein (Figure 2: *pIS*₃) which may provide additional stabilization upon interaction between **18** and the active site of the enzyme. This allows for a different orientation for **18** in the active site, in which interaction with *pIS*₁ is sacrificed in favor of compensatory interaction energy gained via interaction with *pIS*₃. This latter interaction might also be sufficient to activate **18** toward nucleophilic addition of GSH at the *S*-configured carbon atom of the epoxide moiety (*S*-fit). Both the so-called *R*-fit and the *S*-fit of **18** are given in Figure 5, panels a and b, respectively.

Both the number and location of the pyridinyl nitrogen atoms seem to be crucial for the stereoselectivity observed for compounds **14–20** (17). In case no nitrogen atoms are present in the aromatic rings (**14**, **15**), or if they are present at either the 8- or 1-position of the phenanthrene moiety (**16**, **17**), there is no stabilizing interaction favoring the *S*-fit. One nitrogen atom at either the 5- or 4-position of the phenanthrene moiety (**18**, **19**) or a nitrogen at both positions (**20**) enables these substrates to bind in a different orientation in the active site (Figure 5b: *S*-fit). A nitrogen atom at the 5-position of the aromatic system, which is in the same region as the aromatic part of **1** in the *R*-fit (Figure 5a: **18**), seems unfavorable and seems to contribute to directing GSH conjugation to the *S*-configured carbon atom of the epoxide moiety. This is in correspondence with the findings of Cobb *et al.*, who suggested that the loss of stereoselectivity toward phenanthrene 9,10-oxide upon introduction of a nitrogen atom at the 4- and 5-positions is caused by interruption of critical hydrophobic interactions (19). In the case of the azaphenanthrene oxide **19**, GSH conjugation at the *S*-configured carbon atom of the epoxide moiety is still possible (interaction with *pIS*₂), but conjugation at the *R*-configured carbon atom (interactions with both *pIS*₁ and *pIS*₃) is resulting in slightly larger amounts of products conjugated at the *R*-configured carbon atom of the epoxide moiety for **19** than for **18**, which is in correspondence with the findings of Boehlert *et al.* given in Table 1 (17). Introduction of a nitrogen atom at the 1- (**17**) or 8-position (**16**) of the phenanthrene moiety apparently does not disturb aro-

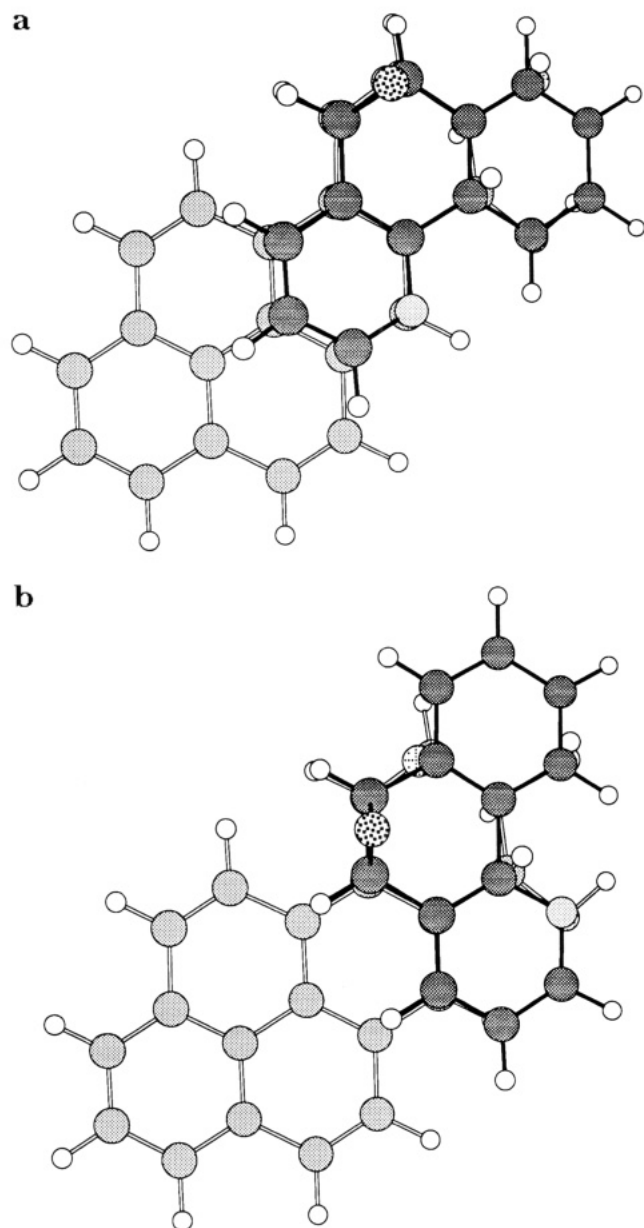


Figure 5. Fits explaining GSH conjugation at the *R*-configured carbon atom of the epoxide moiety (a: *R*-fit) and GSH conjugation at the *S*-configured carbon atom of the epoxide moiety (b: *S*-fit) of **18**.

matic interactions, nor does it attribute to interactions with *pIS*₂ or *pIS*₃. Azaphenanthrene oxide **20** was expected and found (17) to show an intermediate stereoselectivity based on the observation that, in the *S*-fit orientation, interactions with both *pIS*₂ and *pIS*₃ are possible, while in the *R*-fit apart from interactions with *pIS*₁ and *pIS*₂ also a possible destabilizing interaction between the nitrogen atom and the aromatic interaction region (*pIS*₄) is present. All experimentally found relative amounts of products conjugated at the *R*- and *S*-configured carbon atoms of the epoxide moiety (17) can apparently be explained by the present substrate model.

MEPs. Molecular electrostatic potentials (MEPs) generated on the van der Waals surfaces of a series of compounds qualitatively support the proposed substrate model. Evaluation of the MEPs of **1** (Figure 6, upper left panel), **4** (Figure 6, upper right panel), **7**, **14** (Figure 6, lower left panel), and **18**, **19**, and **20** (Figure 6, lower right panel) reveals a number of common features: (1) positive MEP values (>+20 kJ/mol) at the site of attack by GSH;

(2) negative MEP values (<-20 kJ/mol) at the position of the oxygen and nitrogen atoms with Lewis base properties (*IS*₁, *IS*₂, and *IS*₃), involved in interaction with respectively *pIS*₁, *pIS*₂, and *pIS*₃; and (3) negative MEP values (-20 to -10 kJ/mol) in the region of the hydrophobic aromatic ring system of **1**, **14**, **18**, and **19** which is designated *IS*₄. Compounds **18**–**20** have no negative MEP values in the region of the pyridinyl ring, which is supporting the assumption that in the respective *R*-fits an overlap between a nitrogen-containing ring and the aromatic interaction region of the template **1** (*IS*₄) is less favored.

Proposed Substrate Model. The final substrate model derived from the above fit data is proposed to consist of a flat aromatic interaction region (*IS*₄) and three electrostatic interaction sites (*IS*₁, *IS*₂, and *IS*₃) which may function in binding, orientation, and/or catalysis (Figure 2). The distance between the site of GSH attack and *IS*₂ was found to be 3.7 ± 0.1 Å, while the distance between the site of GSH attack and *IS*₃ is 4.3 ± 0.1 Å. The distance between *IS*₂ and *IS*₃ is 2.8 ± 0.1 Å. The three electrostatic Lewis base interaction sites (*IS*₁, *IS*₂, and *IS*₃) correspond with three complementary hypothetical Lewis acid sites in the protein designated *pIS*₁, *pIS*₂, and *pIS*₃ (Figure 2), while the aromatic interaction region (*IS*₄) is proposed to correspond with hypothetical aromatic amino acids in the protein designated *pIS*₄, which may be either above or below the aromatic plane of the model (Figure 2).

Validation of the Substrate Model. The substrate model has been validated by rationalizing the conjugation of 6 substrates, comprising 2 classes of compounds (aromatic epoxides and a nitroso compound) which are known to be metabolized to different extents by GST 4-4 and which were not used in the creation of the substrate model (see Chart 2 and Table 2).

Epoxides (Chart 2). Compounds containing an epoxide moiety next to an aromatic system are good substrates for GST 4-4. Conjugation to GSH preferentially takes place at the benzylic carbon atom of the epoxide moiety with an *R*-configuration (3, 9, 16, 24). Because electronic features of the carbon atoms of the epoxide moiety are identical (in **21**–**23**; data not shown), a relatively rigid catalytically productive orientation of the compound, in the active site of GST 4-4, is likely to be responsible for the high stereoselectivity of the enzyme.

GSH conjugation of *cis*-stilbene oxide **21** by GST 4-4 occurs highly stereoselective ($98 \pm 2\%$) at the *R*-configured carbon atom (16). *trans*-Stilbene oxide is also conjugated by GST 4-4, showing enantioselectivity for *trans*-(*RR*)-stilbene oxide (**22**) over *trans*-(*SS*)-stilbene oxide (**23**) (turnover numbers (*k*_{cat}) 0.12 and 0.023 s⁻¹, respectively (16)). *cis*-Stilbene oxide (**21**) and *trans*-(*RR*)-stilbene oxide (**22**) could be fitted into the present substrate model, in conformations 5.3 and 5.5 kJ/mol, respectively, above their minimal energy conformation (ΔE ; Table 2). The epoxide oxygen atom (*IS*₁), the site of GSH attack, and the aromatic interaction region (*IS*₄) were matched with the corresponding regions in the template molecule **1**. *trans*-(*SS*)-Stilbene oxide (**23**) could only be fitted onto **1** matching *IS*₁ and conjugation sites. It was impossible, however, to superimpose the aromatic regions of **23** and **1**. The additional stabilizing aromatic interaction (*IS*₄···*pIS*₄), which is experienced by **21** and **22** and not by **23**, may explain the preference of GST 4-4

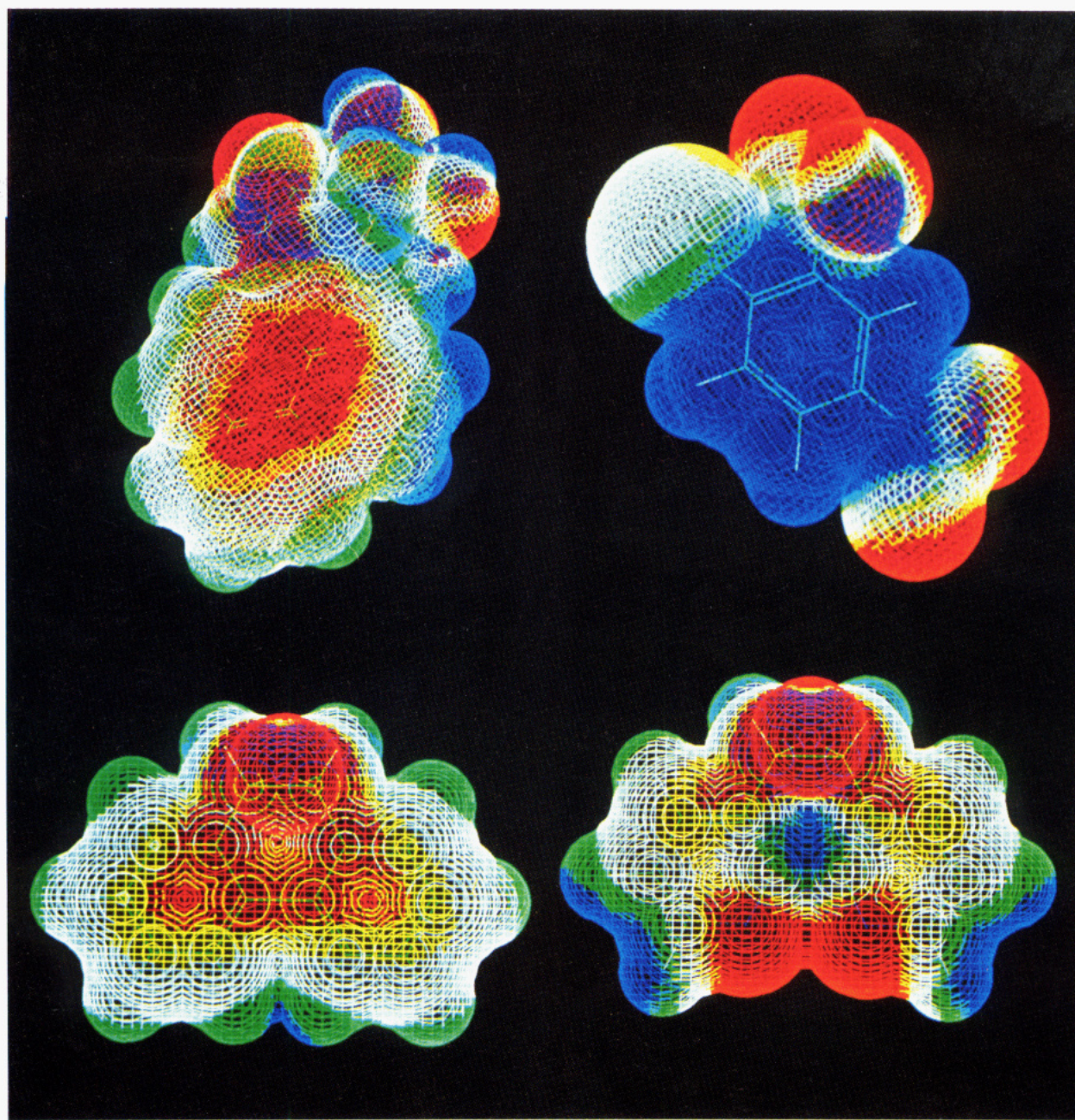


Figure 6. MEPs of **1** (upper left), **4** (upper right), **14** (lower left), and **20** (lower right). MEP colors: red < -20 kJ/mol < yellow < -10 kJ/mol < white < 10 kJ/mol < green < 20 kJ/mol < blue.

for *cis*- and *trans*-(*RR*)-stilbene oxide, when compared to *trans*-(*SS*)-stilbene oxide (16).

GSH conjugation of styrene 7,8-oxide also occurs at the *R*-configured benzylic carbon atom of the epoxide moiety, styrene 7(*R*),8(*S*)-oxide (**24**) being preferred over styrene 7(*S*),8(*R*)-oxide (**25**) with a **24/25** product ratio 1.5 in the case of GST 4-4 (24, 36). Styrene 7(*R*),8(*S*)-oxide (**24**) can be fitted onto **1** in a conformation 6.0 kJ/mol above the minimal energy conformation (ΔE ; Table 2) by matching the epoxide moieties (sites of GSH attack and IS₁) and the aromatic interaction regions (IS₄). Styrene 7(*S*),8-(*R*)-oxide (**25**), however, can only match IS₁ and the site of attack by GSH. As hydrophobic interactions seem to be important for the conjugation of styrene oxide (**24**), the stereoselective conjugation of the styrene oxide enantiomers can be explained with the present substrate model when interactions, with both IS₁ and an aromatic region of the substrate (IS₄), are involved in the orientation, binding, and activation of the compound.

Nitroso Compound (Chart 2). 2-Cyano-1,3-dimethyl-1-nitrosoguanidine (**26**) is known to be conjugated to GSH by GST 4-4 (37) with a specific activity comparable to that of **4**. The reaction catalyzed is a nucleophilic substitution reaction resulting in denitrosation. GSH conjugation can be accounted for by the present substrate model for GST 4-4, by matching the nitroso nitrogen atom (conjugation site of **26**) with the conjugation site of **1** and the Lewis base nitrogen atom next to the nitrile with the 8-hydroxyl oxygen atom of **1** (IS₂). Two low energy conformations, only differing in the orientation of the nitrile moiety, were fitted into the substrate model and were accepted (Table 2).

Predictions Based on the Substrate Model. α,β -Unsaturated ketones like para-substituted 4-phenyl-3-but-en-2-ones (PBOs) **27–31** (Chart 3) were reported to be substrates for GST 4-4 (22, 38). The PBOs are prochiral substrates and are stereoselectively conjugated to GSH by GST 4-4 through a 1,4-Michael addition

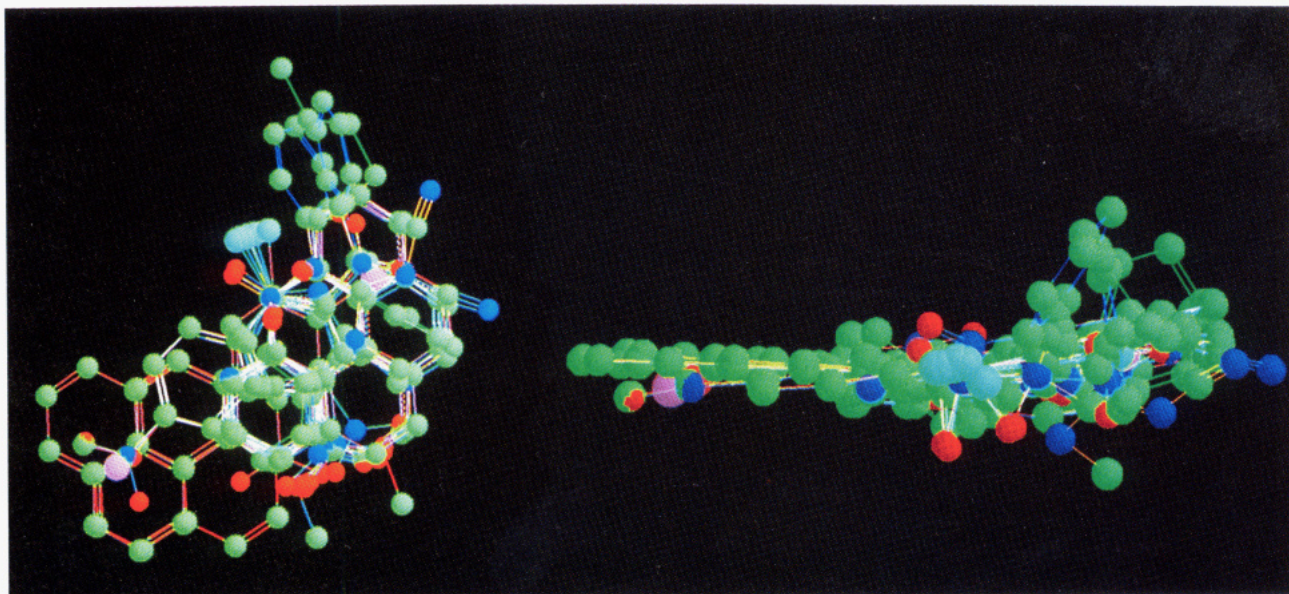


Figure 7. Superposition of all substrates of GST 4-4 used in this study. Hydrogen atoms have been omitted. Top view (left panel) and side view (right panel).

reaction. A correlation was found between the stereoselectivity of the conjugation reaction and the electronic character of the para substituent. The absolute configuration of the GSH conjugated products, however, is unknown (22).

Predictions were made for the compounds depicted in Chart 3. The experimental and calculated data concerning these compounds are given in Table 3. Both the *cis*- and *trans*-conformation of **27** were computationally investigated, showing that the *cis*-conformation is 6 kJ/mol lower in energy than the *trans*-conformation, probably because of steric repulsion between the 2-methyl hydrogen atoms and the hydrogen atom at the β -carbon atom of the α,β -unsaturated system in the *trans*-conformation. This energy difference, however, is not large enough to exclude the *trans*-conformation. Only the *trans*-conformation can be fitted well into the substrate model by matching conjugation sites and superimposing the carbonyl oxygen atom onto the 8-hydroxyl oxygen atom of **1** (IS₂; Figure 2). According to the present substrate model, the GSH conjugate with *R*-configuration, resulting from the *trans*-conformation of the substrate orientated with the *R*-prochiral face of the enone toward the GS⁻ nucleophile, is favored. In our model the aromatic ring of **27** (and therefore also of compounds **28–31**) is coplanar with the aromatic system of **1** (Figure 8: white structure). This aromatic interaction is missing when the *S*-prochiral face of the enone is pointing toward GSH (Figure 8: dark gray structure). The fit resulting in the GSH conjugate with *R*-configuration also explains the diminished stereoselectivity (22) when the para substituent becomes more hydrophilic. A hydrophilic para substituent (e.g., NO₂ in **30**) in the aromatic interaction region of the template **1** (IS₄) is unfavorable when compared to a hydrophobic para substituent (e.g., CH₃ in **29**). The MEP of **27** also shows a large negative value at the carbonyl oxygen atom (IS₂) and a negative value in the aromatic ring (IS₄) (data not shown). Kubo *et al.* (22) proposed that only a specific orientation of the substrate in the active site of GST 4-4 resulting in attack of GS⁻ on one prochiral face of the enone provides an effective dispersion of charge in the transition state.

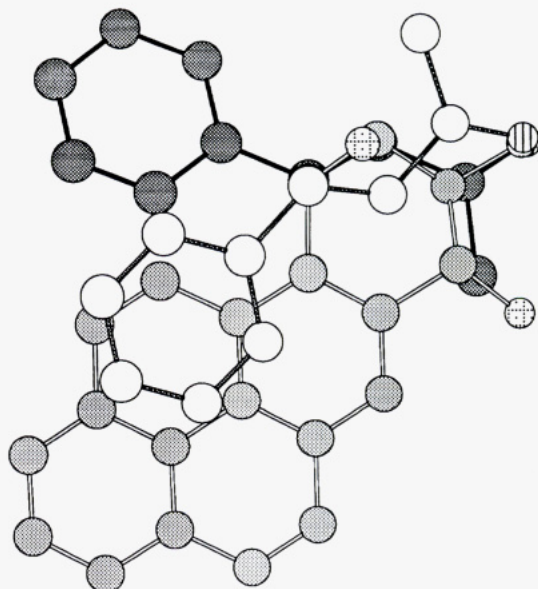


Figure 8. Fits of PBO (27) in the substrate model leading to the *R*-configured GSH conjugate (white) and the *S*-configured GSH conjugate (dark gray). Hydrogen atoms have been omitted.

Substrate Model and Identification of the Interaction Sites. The resulting substrate model including all compounds used is depicted in Figure 7. The hypothetical protein interaction sites as indicated in Figure 2 can be assigned using data from literature.

A recent study of Barycki and Colman revealed Tyr¹¹⁵ to be involved in xenobiotic substrate binding and, with certain types of substrates, in enzymatic catalysis by GST 4-4 (39). When Tyr¹¹⁵ of GST 4-4 was chemically modified with 4-(fluorosulfonyl)benzoic acid, the 1,4-Michael addition reaction of GSH to *trans*-PBO (**27**) and conjugation of GSH to *trans*-stilbene oxide (**22** or **23**) was nearly abolished, while CDNB (**4**) was still conjugated. At neutral pH, Tyr¹¹⁵ is predominantly in a protonated neutral state (39) and thus capable of sharing a proton with an epoxide moiety. Johnson *et al.* found that the hydroxyl group of Tyr¹¹⁵ in the case of GST 3-3 contributes to catalysis of the oxirane ring opening in phenan-

threne 9,10-oxide (14) (40). Furthermore, Ji *et al.* (41) indicated the importance of Tyr¹¹⁵ for the conjugation reaction of 14 and 27 to GSH catalyzed by GST 3-3. Both substrates were suggested to benefit from electrophilic assistance in the stabilization of oxyanions formed by GSH conjugation. Transition state stabilization is small (in GST 3-3 about 10 kJ/mol (41)) but, apparently, enough to substantially affect the catalytic activity of a given isoenzyme toward a given substrate (41). Tyr¹¹⁵ is preserved in GST 4-4 and may have a similar function. In the class alpha glutathione S-transferases, the equivalent to the tyrosine residue (Tyr¹¹⁵) is a valine (Val¹¹¹) (7). Class alpha isoenzymes have a very low specific activity toward aromatic epoxides (3), supporting the relevance of Tyr¹¹⁵ in the catalysis of conjugation of aromatic epoxides to GSH. The first interaction site (*pIS*₁) in the present model of GST 4-4 is therefore proposed to consist of tyrosine residue 115 facilitating epoxide ring-opening reactions (39, 40) and/or binding of substrates (for example, 14). The interaction sites, *pIS*₂ and *pIS*₃, are most likely corresponding to two Lewis acids in the enzyme. In principle, several possibilities exist: two separate acidic amino acids, one flexible acidic amino acid which can cover either of the interaction sites, *pIS*₂ or *pIS*₃, or one semirigid amino acid covering simultaneously interaction site *pIS*₂ and *pIS*₃. For the first two possibilities a flexible charged (or polar) amino acid with one interaction site is a candidate, for example, Lys, Arg, and His. Histidines have been excluded by Zhang *et al.* for GST 3-3 (42). Based on the large homology (88.0% in primary amino acid sequence)² between GST 3-3 and GST 4-4 and the absence of histidine residues near the active site both in human GST subunit 4 (43) and in a preliminary homology model for GST 4-4, histidines can also be ruled out in the case of GST 4-4. An arginine residue can also act as a Lewis acid, which can interact with IS₂ and IS₃ simultaneously. Preliminary homology building studies⁵ have indicated the presence of two arginine residues in the active site of GST 4-4 (Arg⁴² (part of the G-site in GST 3-3 (44)) and Arg¹⁰⁷). None of the three possibilities mentioned above (two separate acidic amino acids, one flexible acidic amino acid which covers *pIS*₂ or *pIS*₃, or one semirigid amino acid which covers *pIS*₂ and *pIS*₃ simultaneously) can be ruled out, however, as arginine is capable of interacting with either one or both of the interaction sites (IS₂ and IS₃).

In the present substrate model 14 is modeled using an interaction with Lewis acid *pIS*₁ (Tyr¹¹⁵), while for 27–31 an interaction with Lewis acid *pIS*₂ is used. These results together with the results of Ji *et al.* (41), who demonstrated that, after mutating Tyr¹¹⁵ to Phe¹¹⁵, the efficiency of conjugation of both 14 and 27 to GSH was diminished, suggest that for some substrates of GST 4-4 the amino acid residues contributing to the hypothetical protein interaction sites *pIS*₁ and *pIS*₂ might be the same. Both the conjugation of 27 and 4 are modeled using *pIS*₂; however, the different behavior of 4 and 27 toward chemical modification of Tyr¹¹⁵ (*pIS*₁) with 4-(fluorosulfonyl)benzoic acid as observed by Barycki and Colman (39) (residual enzyme activity after modification of 4 is 11%, while that of 27 is 2%) cannot be explained, unless the chemical modification of Tyr¹¹⁵ disturbs other interactions in the active site as well. Most likely, *pIS*₁ and *pIS*₂ are different amino acids, but in some reactions Tyr¹¹⁵ (*pIS*₁) might contribute to the interaction of substrates like 27 as would be expected for *pIS*₂.

The nature of the aromatic protein interaction (*pIS*₄) may also be derived from preliminary homology building studies,⁵ which indicated phenylalanine and tyrosine as possible candidates for aromatic interaction sites in the protein (*pIS*₄) complementary with the aromatic regions of the substrates (IS₄).

Conclusions

Based on the regio- and stereoselectivity of GSH conjugation reactions for 20 substrates catalyzed by GST 4-4 (aromatic diol epoxides, aromatic chlorides, pyrene oxide, and (aza)phenanthrene oxides), a substrate model has been developed which comprises the main structural characteristics of substrates of GST 4-4.

Several as yet hypothetical structural elements in the active site of GST 4-4 have been indicated: a flat aromatic region responsible for orientation and stabilization of some substrates, and three other interaction sites consisting of Lewis acid amino acids, one of which is thought to be Tyr¹¹⁵. The Lewis basic atoms in the substrates which interact with other acidic amino acids than Tyr¹¹⁵ are located at distances of 3.7 and 4.3 Å from the site of attack by GSH. The interaction sites are responsible for the orientation, binding, and activation of various substrates. For a series of 2-substituted 1-chloro-4-nitrobenzenes, interaction between a Lewis base atom in the substrate (IS₂/IS₃) and a hypothetical Lewis acidic amino acid in the protein (*pIS*₂/*pIS*₃) is important for activation of the substrate toward nucleophilic substitution and/or for binding of the substrate. Molecular electrostatic potentials of the substrates qualitatively support the substrate model as all substrates exhibit regions with large positive MEP values near the GSH conjugation site, as well as large negative MEP values near the positions of the atoms of the interaction sites (IS₁, IS₂, and IS₃) and in the aromatic region (IS₄).

The substrate model was successfully used to rationalize GSH conjugation of 6 substrates not used to derive the model (styrene oxides, stilbene oxides, and 2-cyano-1,3-dimethyl-1-nitrosoguanidine). Furthermore, predictions were made for some substrates (para-substituted 4-phenyl-3-buten-2-ones) of which GSH conjugation is known to be catalyzed by GST 4-4 with unknown absolute configuration of the products. As all known substrates of GST 4-4 so far can be explained with the present substrate model, this model can be used to qualitatively predict substrates for GST 4-4, similar to what has recently been shown by Koymans *et al.* for substrates of cytochrome P450 2D6 (45). In combination with a protein model of GST 4-4 the present substrate model may be further extended.

Acknowledgment. IBM is gratefully acknowledged for providing RS6000 workstations and NCF (Nederlandse Computer Facilitieiten) for supercomputer facilities.

References

- (1) Armstrong, R. N. (1991) Glutathione S-transferases: reaction mechanism, structure, and function. *Chem. Res. Toxicol.* **4**, 131–140.
- (2) Bladeren, P. J. v., and Ommen, B. v. (1991) The inhibition of glutathione S-transferases: mechanism, toxic consequences and therapeutic benefits. *Pharmacol. Ther.* **51**, 35–46.
- (3) Mannervik, B., and Danielson, U. H. (1988) Glutathione transferases—structure and catalytic activity. *CRC Crit. Rev. Biochem.* **23**, 283–337.
- (4) Mannervik, B., Ålin, P., Guthenberg, C., Jensson, H., Tahir, M. K., Warholm, M., and Jörnvall, H. (1985) Identification of three

⁵ M. J. de Groot *et al.*, unpublished results.

- classes of cytosolic glutathione transferases common to several mammalian species: correlation between structural data and enzymatic properties. *Proc. Natl. Acad. Sci. U.S.A.* **82**, 7202–7206.
- (5) Meyer, D. J., Coles, B., Pemble, S. E., Gilmore, K. S., Fraser, G. M., and Ketterer, B. (1991) Theta, a new class of glutathione transferases purified from rat and man liver. *Biochem. J.* **274**, 409–414.
 - (6) Danielson, U. H., and Mannervik, B. (1985) Kinetic independence of the subunits of cytosolic glutathione transferase from the rat. *Biochem. J.* **231**, 263–267.
 - (7) Sinning, I., Kleynwelt, G. J., Cowan, S. W., Reinemer, P., Dirr, H. W., Huber, R., Gilliland, G. L., Armstrong, R. N., Ji, X., Board, P. G., Olin, B., Mannervik, B., and Jones, T. A. (1993) Structure determination and refinement of human alpha class glutathione transferase A1-1, and a comparison with the mu and pi class enzymes. *J. Mol. Biol.* **232**, 192–212.
 - (8) Mannervik, B., Guttenberg, C., Jakobson, I., and Warholm, M. (1978) Glutathione conjugation: reaction mechanism of glutathione S-transferase A. In *Conjugation reactions in drug biotransformation* (Aitio, A., Ed.) pp 101–110, Elsevier/North-Holland Biomedical Press, Amsterdam.
 - (9) Dostal, L. A., Guttenberg, C., Mannervik, B., and Bend, J. R. (1988) Stereoselectivity and regioselectivity of purified human glutathione transferases π , α - ϵ , and μ with alkene and polycyclic arene oxide substrates. *Drug Metab. Dispos.* **16**, 420–424.
 - (10) Board, P., Coggan, M., Johnston, P., Ross, V., Suzuki, T., and Webb, G. (1990) Genetic heterogeneity of the human glutathione transferases: a complex of gene families. *Pharmacol. Ther.* **48**, 357–369.
 - (11) Roots, I., Brockmöller, J., Drakoulis, N., and Loddenkemper, R. (1992) Mutant genes of cytochrome P-450IID6, glutathione S-transferase class Mu, and arylamine N-acetyltransferase in lung cancer patients. *Clin. Invest.* **70**, 307–319.
 - (12) Comstock, K. E., Widersten, M., Hao, X. Y., Henner, W. D., and Mannervik, B. (1994) A comparison of the enzymatic and physicochemical properties of human glutathione transferase M4-4 and three other human Mu class enzymes. *Arch. Biochem. Biophys.* **311**, 487–495.
 - (13) Ketterer, B., Meyer, D. J., and Clark, A. G. (1988) Soluble glutathione transferase isozymes. In *Glutathione conjugation: Mechanism and biological significance* (Sies, H., and Ketterer, B., Eds.) pp 73–135, Academic Press, Ltd., London.
 - (14) Robertson, I. G. C., and Jernström, B. (1986) The enzymatic conjugation of glutathione with bay-region diol-epoxides of benzo-[α]pyrene, benz[α]anthracene and chrysene. *Carcinogenesis* **7**, 1633–1636.
 - (15) Robertson, I. G. C., Jensson, H., Mannervik, B., and Jernström, B. (1986) Glutathione transferases in rat lung: the presence of transferase 7-7, highly efficient in the conjugation of glutathione with the carcinogenic (+)-7 β ,8 α -dihydroxy-9 α ,10 α -oxy-7,8,9,10-tetrahydrobenzo[α]pyrene. *Carcinogenesis* **7**, 295–299.
 - (16) deSmidt, P. C., McCarrick, M. A., Darnow, J. N., Mervic, M., and Armstrong, R. N. (1987) Stereoselectivity and enantioselectivity of glutathione S-transferase toward stilbene oxide substrates. *Biochem. Int.* **14**, 401–408.
 - (17) Boehlert, C. C., and Armstrong, R. N. (1984) Investigation of the kinetic and stereochemical recognition of arene and azaarene oxides by isozymes A₂ and C₂ of glutathione S-transferase. *Biochem. Biophys. Res. Commun.* **121**, 980–986.
 - (18) Chen, W. J., deSmidt, P. C., and Armstrong, R. N. (1986) Stereoselective product inhibition of glutathione S-transferase. *Biochem. Biophys. Res. Commun.* **141**, 892–897.
 - (19) Cobb, D., Boehlert, C., Lewis, D., and Armstrong, R. N. (1983) Stereoselectivity of isozyme C of glutathione S-transferase toward arene and azaarene oxides. *Biochemistry* **22**, 805–812.
 - (20) Graminski, G. F., Zhang, P., Sesay, M. A., Ammon, H. L., and Armstrong, R. N. (1989) Formation of the 1-(S-glutathionyl)-2,4,6-trinitrocyclohexadienate anion at the active site of glutathione S-transferase: evidence for enzymic stabilization of σ -complex intermediates in nucleophilic aromatic substitution reactions. *Biochemistry* **28**, 6252–6258.
 - (21) Chen, W. J., Graminski, G. F., and Armstrong, R. N. (1988) Dissection of the catalytic mechanism of isozyme 4-4 of glutathione S-transferase with alternative substrates. *Biochemistry* **27**, 647–654.
 - (22) Kubo, Y., and Armstrong, R. N. (1989) Observation of a substituent effect on the stereoselectivity of glutathione S-transferase toward para-substituted 4-phenyl-3-butene-2-ones. *Chem. Res. Toxicol.* **2**, 144–145.
 - (23) Koppele, J. M. te, Coles, B., Ketterer, B., and Mulder, G. J. (1988) Stereoselectivity of rat liver glutathione transferase isoenzymes for α -bromoisovaleric acid and α -bromoisovalerylurea enantiomers. *Biochem. J.* **252**, 137–142.
 - (24) Dostal, L. A., Aitio, A., Harris, C., Bhatia, A. V., Hernandez, O., and Bend, J. R. (1986) Cytosolic glutathione S-transferases in various rat tissues differ in stereoselectivity with polycyclic arene and alkene oxide substrates. *Drug Metab. Dispos.* **14**, 303–309.
 - (25) Cambridge Crystallographic Data Centre, CSD (Cambridge Structural Database), version 3.1, 1988.
 - (26) Chemical Design Ltd., ChemX, version January 1990, 1990.
 - (27) Dupuis, M., Spangler, D., and Wendoloski, J., NRCC Program No. QG01 (GAMESS), 1980.
 - (28) Guest, M. F., Lenthe, J. H. v., Kendrick, J., Schoffel, K., Sherwood, P., Harrison, R. J., with contributions from Amos, R. D., Buenker, R. J., Dupuis, M., Handy, N. C., Hillier, I. H., Knowles, P. J., Bonacic-Koutecky, V., Niessen, W. v., Saunders, V. R., and Stone, A. J., GAMESS-UK, IBM RS6000 v2.1, 1993.
 - (29) Hehre, W. J., Stewart, R. F., and Pople, J. A. (1969) Self consistent molecular orbital methods. I. Use of Gaussian expansions of Slater-type atomic orbitals. *J. Chem. Phys.* **51**, 2657–2664.
 - (30) Stone, A. J. (1981) Distributed multipole analysis, or how to describe a molecular charge distribution. *Chem. Phys. Lett.* **83**, 233–239.
 - (31) Binkley, J. S., Pople, J. A., and Hehre, W. J. (1980) Self consistent molecular orbital methods. 21. Small split-valence basis sets for first-row elements. *J. Am. Chem. Soc.* **102**, 939–947.
 - (32) Gordon, M. S., Binkley, J. S., Pople, J. A., Pietro, W. J., and Hehre, W. J. (1982) Self consistent molecular orbital methods. 22. Small split-valence basis sets for second-row elements. *J. Am. Chem. Soc.* **104**, 2797–2803.
 - (33) Chemical Design Ltd., ChemX, version January 1993, 1993.
 - (34) Carey, F. A., and Sundberg, R. J. (1984) Conformational, steric, and stereoelectronic effects. In *Advanced Organic Chemistry* (Carey, F. A., and Sundberg, R. J., Eds.) pp 118–124, Plenum Press, New York.
 - (35) Eliel, E. L., and Schroeter, S. H. (1965) Conformational analysis. IX. Equilibrations with Raney nickel. The conformational energy of the hydroxyl group as a function of solvent. *J. Am. Chem. Soc.* **87**, 5031–5038.
 - (36) Hiratsuka, A., Yokoi, A., Iwata, H., Watabe, T., Satoh, K., Hatayama, I., and Sato, K. (1989) Glutathione conjugation of styrene 7,8-oxide enantiomers by major glutathione transferase isoenzymes isolated from rat livers. *Biochem. Pharmacol.* **38**, 4405–4413.
 - (37) Jensen, D. E., and Mackay, R. L. (1990) Rat, mouse and hamster isozyme specificity in the glutathione transferase-mediated denitrosation of nitrosoguanidinium compounds. *Cancer Res.* **50**, 1440–1448.
 - (38) Danielson, U. H., Esterbauer, H., and Mannervik, B. (1987) Structure–activity relationships of 4-hydroxyalkenals in the conjugation catalysed by mammalian glutathione transferases. *Biochem. J.* **247**, 707–713.
 - (39) Barycki, J. J., and Colman, R. F. (1993) Affinity labeling of glutathione S-transferase, isoenzyme 4-4, by 4-(fluorosulfonyl)-benzoic acid reveals Tyr¹¹⁵ to be an important determinant of xenobiotic substrate specificity. *Biochemistry* **32**, 13002–13011.
 - (40) Johnson, W. W., Liu, S., Ji, X., Gilliland, G. L., and Armstrong, R. N. (1993) Tyrosine 115 participates both in chemical and physical steps of the catalytic mechanism of a glutathione S-transferase. *J. Biol. Chem.* **268**, 11508–11511.
 - (41) Ji, X., Johnson, W. W., Sesay, M. A., Dickert, L., Prasad, S. M., Ammon, H. L., Armstrong, R. N., and Gilliland, G. L. (1994) Structure and function of the xenobiotic substrate binding site of a glutathione S-transferase as revealed by X-ray crystallographic analysis of product complexes with the diastereomers of 9-(S-glutathionyl)-10-hydroxy-9,10-dihydrophenanthrene. *Biochemistry* **33**, 1043–1052.
 - (42) Zhang, P., Graminski, G. F., and Armstrong, R. N. (1991) Are the histidine residues of glutathione S-transferase important in catalysis? An assessment by ¹³C NMR spectroscopy and site-specific mutagenesis. *J. Biol. Chem.* **266**, 19475–19479.
 - (43) Penington, C. J., and Rule, G. S. (1992) Mapping the substrate-binding site of a human class mu glutathione transferase using nuclear magnetic resonance spectroscopy. *Biochemistry* **31**, 2912–2920.
 - (44) Ji, X., Zhang, P., Armstrong, R. N., and Gilliland, G. L. (1992) The three-dimensional structure of a glutathione S-transferase from the mu gene class. Structural analysis of the binary complex of isozyme 3-3 and glutathione at 2.2-Å resolution. *Biochemistry* **31**, 10169–10184.
 - (45) Koymans, L. M. H., Vermeulen, N. P. E., van Acker, S. A. B. E., te Koppele, J. M., Heykants, J. J. P., Lavrijzen, K., Meuldermans, W., and Donné-Op den Kelder, G. M. (1992) A predictive model for substrates of cytochrome P-450-debrisoquine (2D6). *Chem. Res. Toxicol.* **5**, 211–219.